CHLORIDE ION BINDING ABILITY OF CALCIUM-ALUMINATE, -FERRITE AND -SILICATE PHASES

György BALÁZS, Jolán CSIZMADIA and Károly KOVÁCS

Department of Building Materials
Technical University of Budapest
H–1521 Budapest, Hungary

Abstract

The chloride ion binding ability of C_3A, C_4AF and C_3S clinkers was examined, with special attention to NaCl used for road defrostation. Through thermal analysis and X-ray diffraction investigations it was found that chlorides are bound by C_3A and C_4AF in the form of $3\,CaO \cdot Al_2O_3 \cdot CaCl_2 \cdot 10H_2O$. Calcium-chloro-aluminate-hydrate formed as a result of NaCl even in already settled cement samples. No sign of calcium-chloro-silicate-hydrate was detected by either thermal analysis or X-ray diffraction analysis.

Keywords: chloride binding, clinker minerals.

1. Introduction

Calcium-chloride was used to accelerate the binding and hardening of cement even before the turn of the century. In 1897 Friedel already observed that $CaCl_2$ is bound by the tricalcium-aluminate (C_3A) clinker mineral of cements in the form of the salt:

$$C_3A \cdot CaCl_2 \cdot H_{10}$$

named after him [1].

Since then incredible amount of researches has been executed to make clear what role clinker minerals play during the binding process of $CaCl_2$ [2 – 4]. In the following we discuss some works from the literature.

Most researchers proved the formation of Friedel-salt in the C_3A–$CaSO_4$–$CaCl_2$ system [5 – 9]. Friedel salt is one of the most stabilized hydrates, unlike $C_3A \cdot 3CaCl_2 \cdot H_{30}$ that is only formed under certain circumstances and is unstable. Both $CaSO_4$ and $CaCl_2$ react with C_3A. While certain researchers consider the generation of ettringite ($C_3A \cdot CaSO_4 \cdot H_{31}$) as the primer step [5], Balázs and Boros keep [10] that Friedel salt precedes it, as while $CaCl_2$ is mixed into the paste as a solution, gypsum is mixed as a solid material, therefore it has to be dissolved first. The amount of

the formed hydrates is affected by the proportions of the original materials, and by the preparation and storage circumstances.

Some researchers suppose that another hydrate $(C_3F \cdot CaCl_2 \cdot H_{10})$ like Friedel salt is formed from C_4AF [11].

One part of the researchers supposes that C_3S does not react with $CaCl_2$, but $CaCl_2$ accelerates the forming of CSH-hydrates.

The above mentioned thoughts refer to that particular case when $CaCl_2$ is added to the mixing water. Wintertime salt treatment of roads brings up a new problem, whether NaCl used as a defrostation salt is able to build into the already hardened cement stone. This phenomenon was hardly ever examined in the case of clinker minerals. The goal of this research was to contribute to the explanation of the formation circumstances of subsequent chloride binding.

2. Experiments

The significant amount of relevant literature on chloride binding ability of clinkers mostly discusses what quantity the cements bind from $CaCl_2$ added to the mixing water and how. It is generally presumed that chloride ion is bound primarily by the tricalcium aluminate: $3CaO \cdot Al_2O_3$ (C_3A) clinker mineral of cements. We examine this compound first. *Table 1* shows the scheme of the investigation.

Samples of $10 \times 10 \times 50$ mm were prepared and stored in atmospheres of 100 and 65% relative humidity at a temperature of $20 \pm 3°C$. The effect of steaming was also stone. This examined by storing samples at 80 °C for 6 hours after their preparation. In case of samples containing NaCl the salt was added to the mixing water, while in the case of other samples the following treatments were used (modelling the effects of salt used for wintertime road defrostation):

Procedure 1: we sprayed salt solution on the samples daily between 1 – 28 days, during 1 minute;

Procedure 2: the same as No. 1 but between 28 – 56 days;

Procedure 3: we spilled salt solution on the samples daily between 1 – 28 days;

Procedure 4: the same as No. 3 but between 28 – 56 days;

Procedure 5: we stored the samples in salt solution between 1 – 28 days;

Procedure 6: the same as No. 5 but between 28 – 56 days.

The concentration of the salt solution was 100 g/l. The column-shaped samples made us possible to have a strength analysis record for every chemical investigation by cutting 1 cm slices from the columns.

Table 1

The composition of samples and the circumstances of investigation

Mark	C_3A g	Gypsum g	H_2O g	NaCl g	Temperature °C	Mark of salt treatment	Vapour content %
1	20	–	16.0	–	20	–	ethalon 100
2	20	6(30%)	20.8(0.8)	–	20	–	ethalon 100
3	20	6(30%)	20.8(0.8)	–	20	–	ethalon 65
4	20	6	20.8	–	80; 6 hours	–	ethalon 100
5	20	6	20.8	–	80; 6 hours	–	ethalon 65
6	20	4(20%)	19.2(0.8)	–	20	–	ethalon 100
7	20	–	16	0.4	20	–	100
8	20	6	20.8	0.4	20	–	100
9	20	6	20.8	–	20	1	100
10	20	6	20.8	–	20	2	100
11	20	6	20.8	–	80; 6 hours	1	100
12	20	6	20.8	0.4	20	1	65
13	20	6	20.8	–	20	1	65
14	20	6	20.8	–	20	3	100
15	20	6	20.8	–	20	3	65
16	20	6	20.8	–	20	4	100
17	20	6	20.8	–	80; 6 hours	3	100
18	20	6	20.8	–	20	5	100
19	20	6	20.8	–	80; 6 hours	5	100
20	20	6	20.8	–	20	6	100

The investigations took place at the ages of 1, 28, 56, 90 and 180 days. Investigation procedures:

a) thermal and X-ray diffraction analysis,
b) splitting strength analysis.

Features of the derivatograph:

type	MOM Q-1500D
reference material	Al_2O_3
sample weight	170±20 mg
crucible	corundum
heating rate	10 °C/min
temperature range	20 – 980 °C
sensibility	0.5 mg/grade
atmosphere	air

Features of the X-ray diffractometer:

type	JEOL, JDX 85
X-ray tube	Cu K_α
accelerating voltage	40 kV

anode current strength   40 mA
sensibility $1 \cdot 10^3$ c/s
goniometer speed   2 degrees/min (Θ)
paper speed   20 units/min

3. Results and Evaluation

3.1. C_3A–Water System (Table 1, experiment 1)

The main product of the C_3A–water reaction is tricalcium-aluminate-hexahydrate: $3CaO \cdot Al_2O_3 \cdot 6H_2O$ (C_3AH_6) [2, 3]. As a result of heating, C_3AH_6 loses its 6 mole crystal water in two steps showed by the peaks at 280 and 450 °C on the DTG curve of the derivatogram on *Fig. 1*. Apart from humidity evaporating until 100 °C, the derivatogram shows certain loss of weight between 100 – 160 °C, originating from dicalcium-aluminate-octahydrate: $2CaO \cdot Al_2O_3 \cdot 8H_2O$ (C_2AH_8) and tetracalcium-aluminate-dodecahydrate: $3CaO \cdot Al_2O_3 \cdot Ca(OH)_2 \cdot 12H_2O$ (C_4AH_{13}). The peak of 160°C is increasing compared to the peak of C_3AH_6 as hydration proceeds. This corresponds to the latest experimental results [12], showing that C_4AH_{13} is a stable compound. It was earlier accepted that C_2AH_8 and C_4AH_{13} appearing at the beginning of the hydration process are 'unstable' hexagonal calcium-aluminate-hydrates, which soon transform into C_3AH_6 – that has a regular (cubic) structure – under the following reaction:

$$C_2AH_8 + C_4AH_{13} = 2C_3AH_6 + 9H.$$
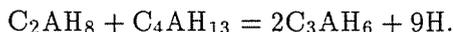
The DTG peak at 280 °C has a 'shoulder' around 220 °C, that originates from $Al(OH)_3$ (AH_3) according to the following equation:

$$\frac{3}{2}C_2AH_8 = C_3AH_6 + \frac{1}{2}AH_3 + 9\left(\frac{1}{2}H\right).$$
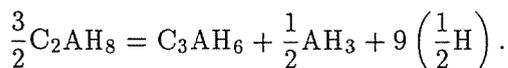
X-ray diffraction analysis detected small quantities of C_4AH_{13}, mixture of dicalcium- and tetracalcium-aluminate-hydrate (C_3AH_{8-12}), original C_3A and portlandite: $Ca(OH)_2$ besides C_3AH_6 in the 180-day-old sample (*Fig. 2a*)

3.2. C_3A–Water–NaCl System (Table 1, experiment 7)

In case of C_3A with 1.1 per cent of NaCl added to the mixing water the product of the hydration process was similar to the samples without NaCl (*Table 2*), but the shoulders of the DTG curve (120 °C, 225 °C) were
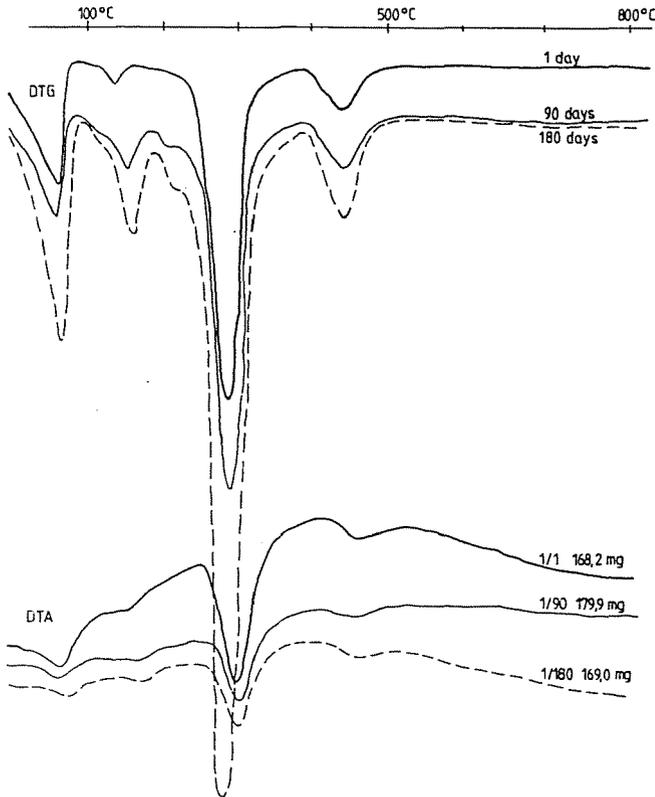
Fig. 1. DTG and DTA curves for C_3A–water samples of different ages

hardly to be detected; the water content and the loss of weight around 150 °C increased during hydration. The formation of a chlorous hydrate: $3CaO \cdot Al_2O_3 \cdot CaCl_2 \cdot 10H_2O$ ($C_3A \cdot CaCl_2 \cdot H_{10}$; Friedel salt) seems possible according to the X-ray diffraction spectrum (*Fig. 2b*) though no sign of it should be found on the derivatogram.

3.3. $C_3A–CaSO_4 \cdot 2H_2O–Water\ System$

The main product of the C_3A+gypsum+water reaction (*Table 1*, experiment 2) after 1 day is tricalcium-aluminate-monosulphate-hydrate: $C_3A \cdot CaSO_4 \cdot H_{12}$: /$C_4A\bar{S}H_{12}$/ peak around 190 °C on the DTG curve. There are two shoulders on this peak (*Fig. 3*). The first shoulder at 140 °C is caused by ettringite: $C_3A \cdot 3CaSO_4 \cdot H_{32}$ formed in the beginning of the process. The second one at 170 °C belongs to C_4AH_{13}.

GY. BALÁZS et al.

A – C$_3$A
H6 – C$_3$AH$_6$
H8 – C$_2$AH$_8$
H13– C$_4$AH$_{13}$
C – calcit
P – portlandit

H6, 1,63
H6, 1,74

H8, 1,62

C, 1,91
H8, 1,93

H6, 2,04

H6, 2,30

A,H6, 2,47   A 2,42

A,H6 2,70

H6 2,81

H6 3,14   C 3,04

H6 3,37

H8 3,79

H6 4,45

H6   5,16

H8 7,65   H13 7,10

A – C$_3$A
H6 – C$_3$AH$_6$
H13– C$_4$AH$_{13}$
F – C$_3$A·CaCl$_2$·10H$_2$O
P – portlandit
C – calcit

H13,F 1,62
H13,H6 1,71
H6 1,74
H6 1,63

H6 2,04

F 2,11   C 2,09

H6 2,30

H13   F 2,87

F 2,52

H6 , H13 2,81   F,H13 2,87   C 3,03

H6,P 3,14

H6 3,36

F 3,80
H13,F 3,90   A 4,08

H6 4,45

F 4,89

H6 5,16

F,H13 7,23

Fig. 2. X ray diffraction spectrum of 180 day-old C$_3$A–water sample. a) C$_3$A–water; b) C$_3$A water NaCl
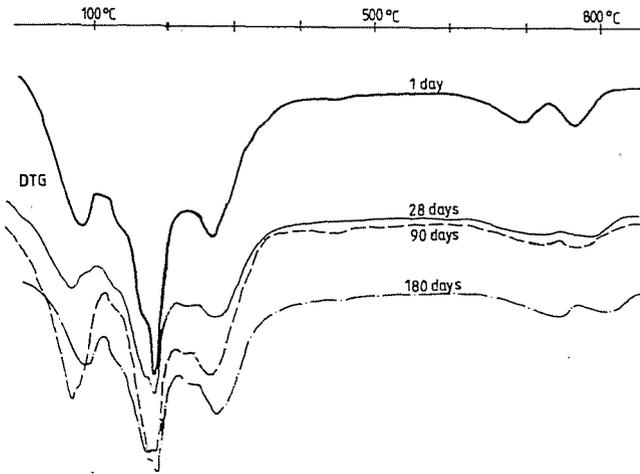
Fig. 3. DTG curves for C_3A–gypsum–water samples of different ages
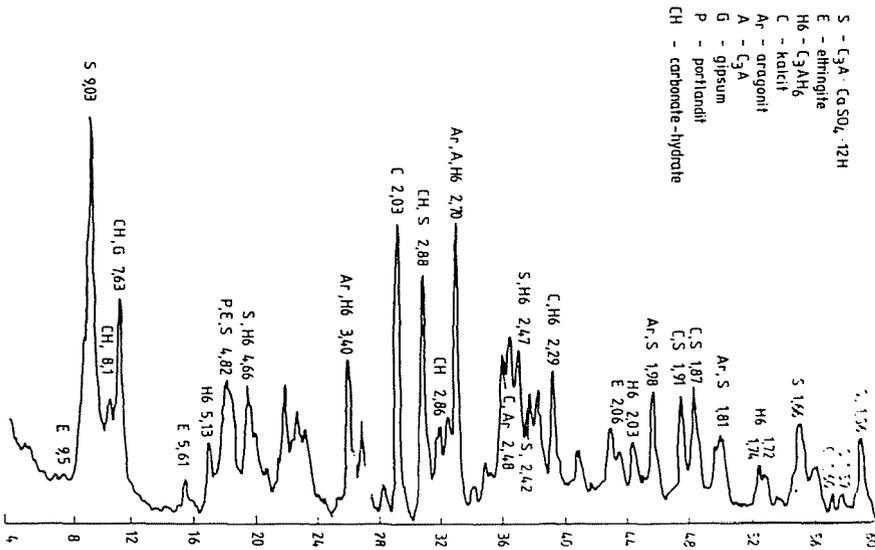
Fig. 4. X-ray diffraction spectrum of 250 day old C_3A gypsum water sample

Pure monosulphate is rarely found, as it forms solid solution with C_4AH_{13} at room temperature.
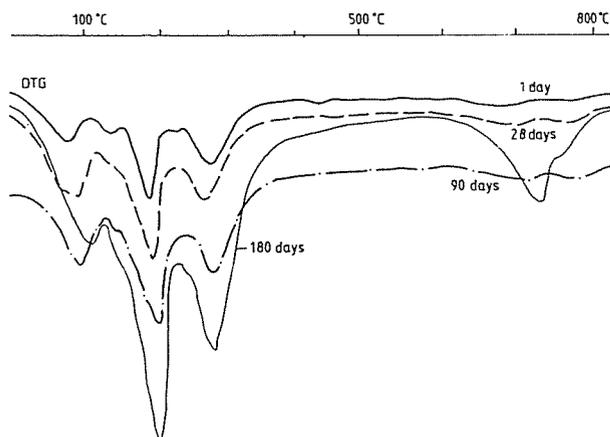
Fig. 5. DTG curves for steamed C_3A-gypsum-water samples of different ages
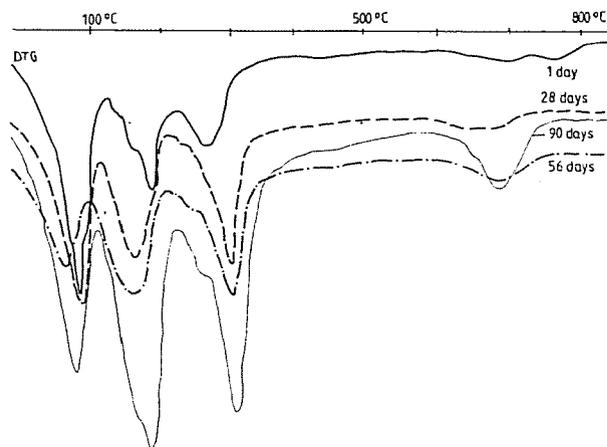
Fig. 6. DTG curves for C_3A–gypsum–water samples of different ages stored in 10% NaCl solution between 1 – 28 days

The peak appeared at 290 °C belongs to the C_3AH_6, but the AF_m phases (C_4AH_{13}, $C_4A\overline{S}H_{12}$) and ettringite lose water around this temperature, too.
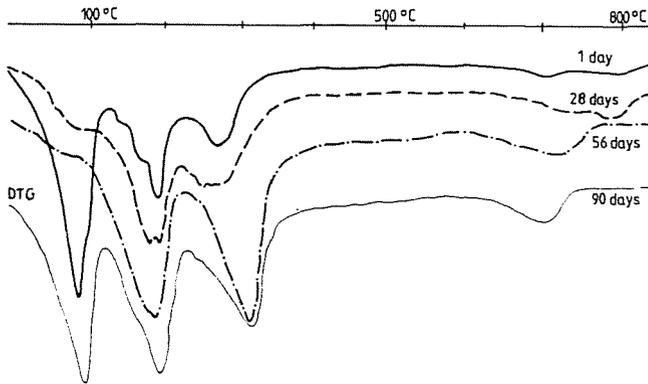
Fig. 7. DTG curves for C_3A–gypsum–water samples of different ages stored in 10% NaCl solution between 28 – 56 days

The peaks of the DTG curve widened over the age of 28 days, showing the increasing possibility of reactions between the produced compounds. The shoulder at 230 °C probably belongs to AH_3. The peaks at 700 and 770 °C show the CO_2 loss from carbonates.

The effect of gypsum on holding back C_3A hydration mentioned by [13] was not observed.

X-ray diffraction analysis detected monosulphate, ettringite, C_3AH_6, C_4AH_{13}, C_3A, portlandite and $CaCO_3$. The formation of calcium-aluminate-carbonate-hydrate: $C_3A \cdot CaCO_3 \cdot H_{11}$ and calcium-aluminate-hemicarbonate-hydrate: $C_3A \cdot 1/2Ca(OH)_2 \cdot 1/2CaCO_3 \cdot H_{11.5}$ also seems possible from reflections at 7.63, 3.99, 2.86 Å respectively 8.1, 4.4, 2.88 Å (*Fig. 4*).

The product of the reactions in samples stored in 65% rel. humidity had similar constituents as compared to samples stored in 100% rel. humidity, but the quantities and proportions were different.

Their bound water content was 4 – 5 per cent lower.

In case of the hydration of samples exposed to steam at 80 °C for 6 hours (*Table 1,* experiment 4) the DTG curves of 1-day-old samples show symmetrical, separated peaks without any shoulders. These peaks belong to humidity (around 100 °C), ettringite (140 °C), monosulphate (190 °C) and C_3AH_6 (290 °C) (*Fig. 5*).

Samples stored in 65% relative humidity atmosphere after being steamed had a bound water content 7 – 8 per cent lower than samples stored in 100% relative humidity after steaming (*Table 1,* experiment 5).

When the system had 20% $CaSO_4 \cdot 2H_2O$ content referred to C_3A instead of the given 30% (*Table 1,* experiment 6) the main product of hy-

Table 2

Weight losses of the C_3A samples hydrated under different circumstances (calculated from the TG curves)

	1 day in steam				
	130 – 600 °C	20 – 130 °C	600 – 780 °C	600 – 900 °C	
Mark	bound water	humidity	CO_2	NaCl	$\sum$
			%		
1	16.35	6.24	2.14	-	24.73
7	13.57	8.15	1.93	-	23.65
2	16.98	4.45	2.12	-	23.55
3	15.63	10.04	1.50	-	27.17
4	15.58	3.32	3.75	-	22.65
5	14.66	1.23	3.01	-	18.90
6	14.83	10.66	1.64	-	27.13
8	13.91	13.39	-	2.46	29.76
9	14.44	8.78	2.84	-	26.03
10	13.71	13.70	2.49	-	30.90
11	15.28	0.89	2.42	-	18.59
12	13.63	16.80	-	2.47	32.90
13	8.63	8.4	1.10	-	17.87
14	15.35	12.31	2.40	-	30.04
15	15.59	13.42	2.55	-	31.56
16	16.42	10.03	2.23	-	29.68
17	14.55	0.24	2.72	-	17.51
18	16.42	11.93	2.27	-	30.62
19	14.36	[?]	2.85	-	17.20
20	14.84	11.87	1.97	-	28.68
	28 days in steam				
1					
7	20.42	11.65	1.44	-	33.50
2	21.82	11.42	3.12	-	29.36
3	17.81	3.44	2.15	-	23.40
4	19.40	6.53	3.04	-	28.97
5	15.67	2.08	2.49	-	20.24
6	21.04	9.55	1.44	-	32.17
8	19.17	15.37	-	2.14	36.68
9	18.99	8.73	-	2.67	30.39
10	21.06	10.19	2.14	-	34.39
11	16.39	12.43	-	2.49	31.31
12	19.57	9.64	-	2.70	32.01
13	18.10	4.09	-	2.33	24.52
14	19.34	9.81	-	2.89	32.04
15	17.27	4.16	-	2.60	24.03
16	19.63	7.13	4.07	1.48	29.31
17	16.22	13.07	-	4.02	38.31
18	20.09	10.22	-	2.45	32.76
19	19.08	11.06	-	2.50	38.69
20	21.91	2.78	3.13	-	28.72

Table 2
(Continued 1)

Mark	56 days in steam				
	130 – 600 °C bound water	20 – 130 °C humidity	600 – 780 °C CO_2 %	600 – 900 °C NaCl	$\sum$
1					
7					
2					
3					
4					
5					
6					
8					
9	19.29	7.91	0.96	1.93	30.19
10					
11	18.92	6.76	-	2.71	28.39
12	19.60	12.12	-	2.38	34.24
13	18.73	3.78	-	2.13	24.52
14	[20.04]	11.85	-		[32]
15	17.55	3.37	-	2.95	23.83
16	22.71	6.92	1.08	2.01	31.72
17	17.73	11.55	-	3.65	35.93
18	21.95	6.64	-	2.47	30.90
19	23.76	1.01	-	3.80	28.57
20	22.99	0.90	-	2.37	26.26
	90 days in steam				
1	22.00	4.31	2.14		28.45
7	22.50	8.39	1.60		32.49
2	23.16	8.21	3.21	-	34.58
3	18.53	2.78	2.06	-	23.37
4	22.25	8.05	2.28	-	32.58
5	14.49	1.88	2.68	-	19.00
6	23.51	9.93	2.43	-	35.87
8	20.26	13.00	?	2.36	35.52
9	19.66	9.65	0.52	3.05	32.88
10	21.93	11.83	1.00	1.88	36.58
11	18.76	12.20	-	2.71	33.90
12	19.04	13.15	-	2.36	34.55
13	17.59	3.83	-	2.11	23.52
14	21.10	11.85	-	2.81	35.76
15	18.58	4.23	-	2.42	25.33
16	23.19	6.89	-	3.93	34.01
17	20.16	4.87	-	4.68	30.71
18	23.54	7.38	-	2.74	33.66
19	23.28	7.07	-	3.86	34.21
20	23.01	9.84	-	2.47	34.22

Table 2

(Continued 2)

	180 days in steam				
	130 – 600 °C	20 – 130 °C	600 – 780 °C	600 – 900 °C	
Mark	bound water	humidity	CO_2	NaCl	$\sum$
			%		
1	24.08	5.32	1.78		31.18
7	25.60	4.55	1.66		31.81
2	24.33	4.44	2.93	-	31.70
3	18.68	2.20	2.47	-	23.35
4	21.40	3.95	5.60	-	30.95
5	14.47	1.88	2.62	-	18.97
6	24.71	10.10	2.78	-	37.58
8	24.75	4.69		3.52	32.76
9	22.47	3.53	-	4.71	30.71
10	23.23	9.77	-	4.0	37.0
11	19.00	7.32	-	5.56	31.88
12	21.02	11.23	-	5.0	37.25
13	18.24	4.12	-	3.53	25.84
14	24.00	9.39	-	2.39	35.78
15	21.85	3.86	-	2.69	28.40
16	23.45	6.0	-	4.97	34.42
17	20.19	10.68	-	4.72	35.55
18	23.56	8.08	-	2.72	34.36
19	23.37	[3]	-	5.88	38.35
20	23.78	8.34	-	5.00	37.12

dration was C_3AH_6. The two DTG peaks between 120 – 230 °C were of the same intensity after 1 day, but as the hydration proceeded the quantity of C_4AH_{13} (170 °C) increased, while the peak of monosulphate (190 °C) formed only a shoulder after 28 days. Ettringite (140 °C) could by detected even after 180 days.

3.4. $C_3A-CaSO_4-Water-NaCl$ System (Table 1, experiments 8 – 20)

Samples taken during the hydration process of C_3A–$CaSO_4$–water–NaCl system show less diversity in their DTG curves than the ones with no NaCl content. The DTG peak around 190 °C lost its shoulder of 170 °C after the very first day in case of samples with NaCl added to their mixing water, and after the salt treatment in case of samples sprayed or spilled with NaCl solution. Parallel to this the DTG peak between 230 – 400 °C has widened towards higher temperatures (*Fig. 6*).
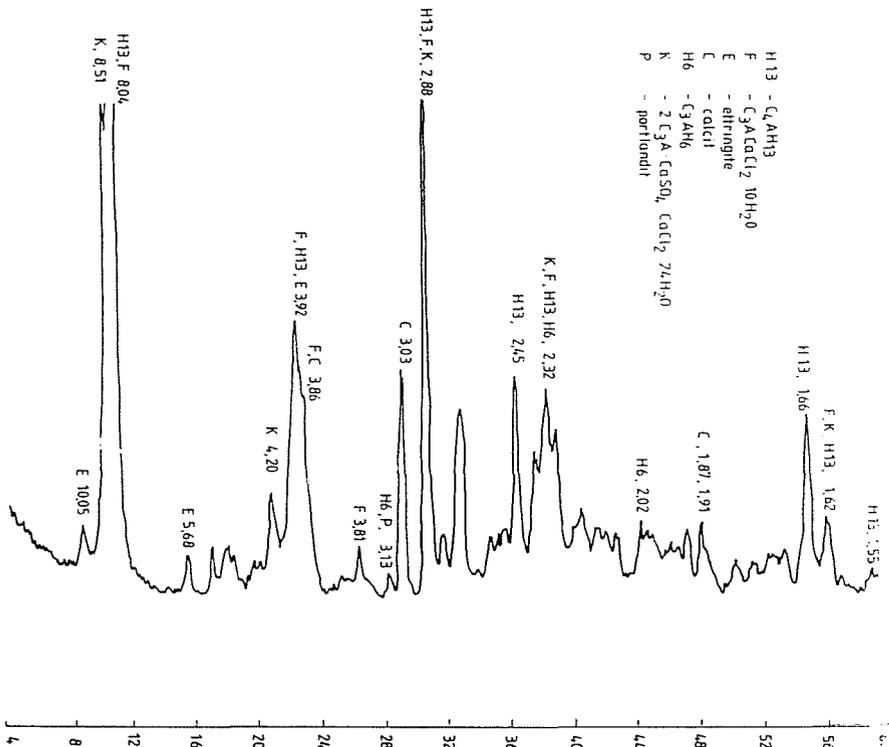
Fig. 8. X-ray diffraction spectrum for 250-day-old C_3A–gypsum–water sample stored in 10% NaCl solution between 28 – 56 days

The shoulder appearing around 300 °C at samples containing NaCl or exposed to salt solution renders the formation of a possible new component. Samples stored in NaCl solution of 10% concentration showed a DTG peak between 230 – 400 °C with a minimum point at 320 °C, which shows significant increase in the concentration of the new component. Our colleagues [10] identified this peak in the case of $C_3A+CaCl_2$ system. The peak appearing at 320 °C belongs to calcium-chloroaluminate-hydrate: $C_3A \cdot CaCl_2 \cdot H_{10}$ (Friedel salt). Friedel salt is stabilised in solutions containing 3 g/l $CaCl_2$, but forms solid solution with C_3AH_{13} in case of lower $CaCl_2$ concentration: $C_3A \cdot 1/2CaCl_2 \cdot 1/2Ca(OH)_2 \cdot H_{12} - C_3A \cdot CaCl_2 \cdot H_{10}$ [11]. The possibility of trichloro-aluminate-hydrate: $C_3A \cdot 3CaCl_2 \cdot H_{30}$ to appear is low due to temperatures over 20 °C and to the low Cl^- concentration [12].

Therefore Cl^- diffusing into the setting cement from salt solution is bound in the form of Friedel salt.

Friedel salt appearing in samples stored in NaCl solution between 28 – 56 days shows that Cl^- can bind into already hardened concretes (*Fig. 7*).

The DTG peak at 170 °C on the derivatogram may belong to C_4AH_{13}, monosulphate, Friedel salt and their solid solutions, the one at 320 °C belongs to Friedel salt and C_3AH_6.

X-ray diffraction analysis identifies the same hydrates (*Fig. 8*).
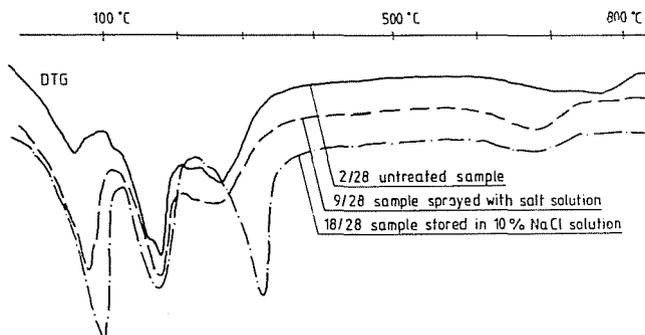
Fig. 9. Results of treatment on DTG curves of 28-day-old C_3A–gypsum–water samples exposed to salt solution between 1 – 28 days

Fig. 9 shows the effect of the hydration circumstances in the case of hydrated (28-day-old) $C_3A+CaSO_4\cdot2H_2O+$water samples.

3.5. Variation in Time of Splitting Strength

The following equation gives us the relation between splitting strength and the splitting force:

$$R_{ts} = \frac{2F}{\pi \cdot d \cdot h},$$

where F is splitting force,

$\quad d$ is diameter of the inside cylinder,

$\quad h$ is length of the splitting plane.

As d and h both are equal to 10 mm we only have to multiply F by the constant $\left(\frac{2}{\pi}0.637\right)$. We summarised the results (splitting force according to age) in a figure. These are only informative results as we only had 1 measurement result for each age.

Conclusion:

a) The strength of C_3A–water system started from a very low level but increased continuously, due to hexagonal calcium-aluminate-hydrates appearing in the beginning of the process constantly transforming into C_3AH_6 (*Fig. 10,* sample 1). The 2% NaCl content related to C_3A approximately doubled the strength (*Fig. 10,* sample 7).
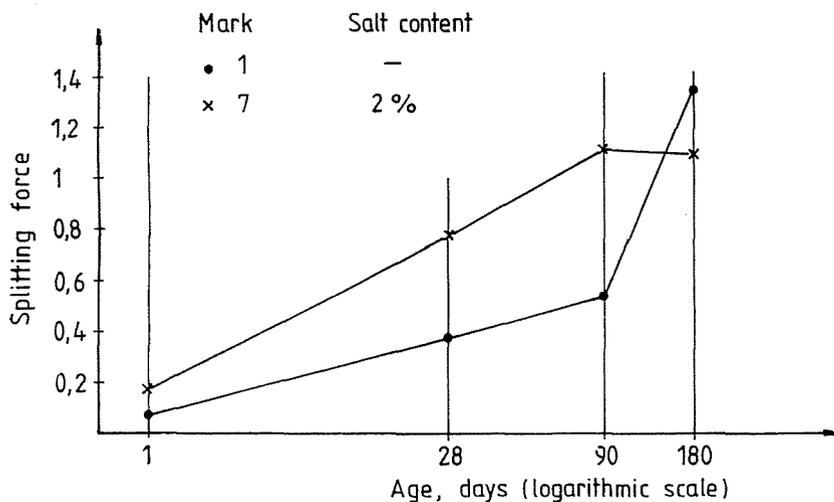
Fig. 10. Settling process of C_3A–water columns
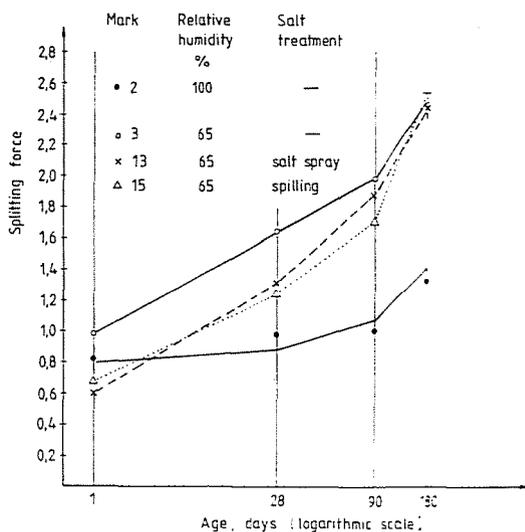
Fig. 11. The effect of humidity and salt treatment on the setting process

b) The original strength of C_3A–gypsum–water system was $4-5$ times higher than it was without gypsum (*Fig. 11,* sample 2, compared to sample 1 in *Fig. 10*). This original strength came mostly from ettringite and monosulphate. After 28 days strength increased slowly
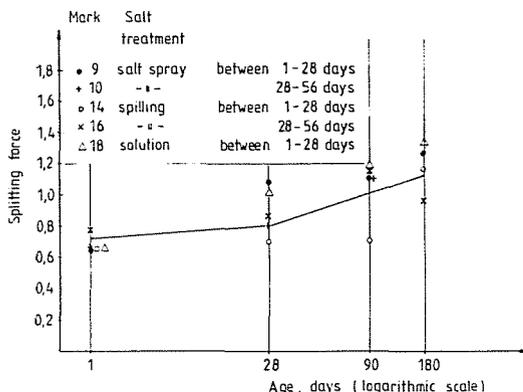
Fig. 12. The effect of salt treatment procedure on the setting process

in the beginning and accelerated later to reach a level around 1.75 times higher by 180 days due to recrystallization.

c) When samples of C_3A–gypsum–water system were exposed to salt solution of 10% concentration either by spraying or spilling between 1–28 or 28–56 days their strength characteristics were similar to samples without exposition to salt (*Fig. 12*, compared to *Fig. 11* mark 2).

d) Samples of C_3A–gypsum–water system stored in 65% relative humidity atmosphere naturally had similar original strength values compared to samples stored in 100% relative humidity, but reached around two times higher levels by 180 days.

   This difference in strength was not affected by exposing the samples to salt (*Fig. 11*, samples 3, 13 and 15, compared to sample 2).

e) Steamed samples of C_3A–gypsum–water system showed relatively high strength after 1 day; this value dropped back later but reached the original level by 180 days. This was not affected by any form of salt treatment (*Fig. 13*). This characteristic is in accordance with the fact that 1-day-old samples already have developed hydrate structure, which hardly ever changes afterwards. The formed Friedel salt had little impact on strength.

3.6. C_4AF–Water System

The most intensive peak on DTG curve (at 170 °C) of hydrated tetracalcium-aluminate-ferrite samples belongs to C_4AH_{13}, C_4FH_{13}, and/or their solid solution. The wide peak between $200 - 300$ °C originates from C_3AH_6, C_3FH_6 and/or their solid solution, while the shoulders on the peak belong
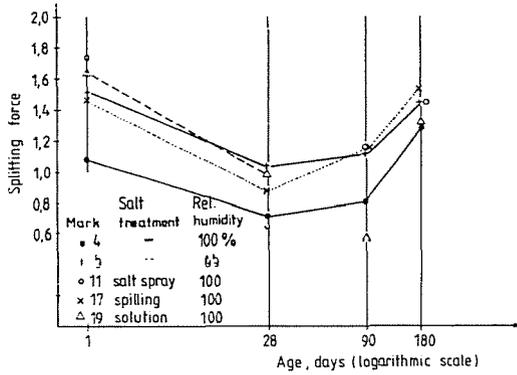
Fig. 13. Setting process of steamed columns under treatment
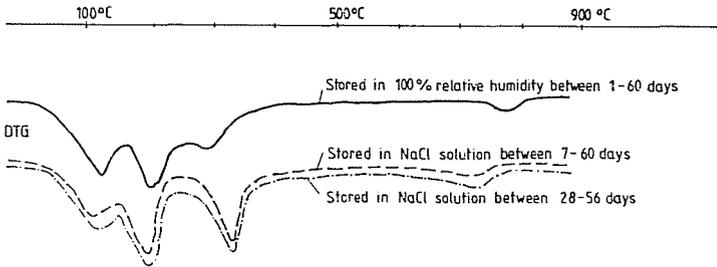
Fig. 14. DTG curves of 60 day-old C_4AF–gypsum–water samples

to metal-hydroxides $Al(OH)_3$, $Fe(OH)_3$ [13] appearing in the beginning phase of the reaction.

The formation rate of the hydrogarnet phase: $(C_3AH_6–C_3FH_6)$ is much lower in C_4AF as compared to C_3A. After 24 hours the hydrogarnet: $C_4AH_{13}–C_4FH_{13}$ ratio is 1:1.27 in case of the hydration of C_4AF; while C_3A hydration has a $C_3AH_6:C_4AH_{13}$ ratio of 14.6:1.

3.7. $C_4AF–CaSO_4–Water$ System

When gypsum is present at the hydration of C_4AF the most intensive DTG peak is again at 200 °C, originating; from hexagonal hydrates C_4AH_{13} and C_4FH_{13} and monosulphates $C_3A \cdot CaSO_4 \cdot H_{12}$, $C_3F \cdot CaSO_4 \cdot H_{12}$. Sulphoalu-
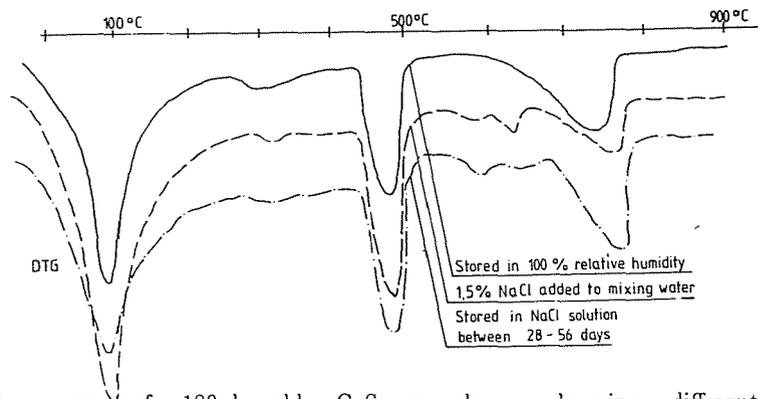
Fig. 15. DTG   curves   of   180-day-old C_3S samples   undergoing   different
        hydration procedures

minate phase forms solid solution with the analogous sulphoferrite phase
[7], though not under every concentration ratio.

Ettringite and C_3AH_6–C_3FH_6 are probably present.

3.8. C_4AF–$CaSO_4\cdot 2H_2O$–Water–$NaCl$ System

In case of samples containing $CaSO_4$+$NaCl$ a DTG peak at 325 °C was
detected in samples stored in NaCl sol. between either 7 – 60 or 28 –
60 days. This peak belongs to $C_3A\cdot CaCl_2\cdot H_{10}$, $C_3F\cdot CaCl_2\cdot H_{10}$ and/or their
solid solution.

Therefore C_4AF binds chlorides similarly to C_3A, in the form of
Friedel salt (*Fig. 14*).

3.9. C_3S–Water System

We investigated the chloride binding ability of tricalcium–silicate:
$3CaO\cdot SiO_2$ (C_3S) by the experiment scheme shown in *Table 3*. The num-
bers for salt treatment mark the same procedures as listed at C_3A.

The peaks on the similar DTG curves of C_3S samples undergoing
different hydration procedures belong to the following processes (*Fig. 15*).

The peak between 40 – 400 °C with a minimum temperature at 100 °C
includes adsorbed humidity, some parts of the pore water and most of the
interlayer water. These different water types constantly evaporate from the
material as temperature increases. Smaller peaks at 300, 500 and 630 °C
show the loss of structural water. Absorbed water can not be completely
separated from the structural water [14].

Table 3
Experiments with C_2S

Mark	C_3S g	H_2 g	NaCl g	Temperature °C	Mark of salt treatment	Relative humidity %
1	10	3	–	20	–	ethalon 100
2	10	3	–	20	–	ethalon 65
3	10	3	–	60; 4 hours	–	ethalon 100
4	10	3	0.2	20	–	100
5	10	3	–	20	1	100
6	10	3	–	20	2	100
7	10	3	–	20	3	100
8	10	3	–	20	4	100
9	10	3	–	20	6	100
10	10	3	–	20	5	100
11	10	3	0.2	20	3	100
12	10	3	0.2	20	4	100
13	10	3	–	60; 4 hours	3	100
14	10	3	–	60; 4 hours	4	100

The hydration reaction of C_3S may be described by the following equation:

$$3CaO \cdot SiO_2 + (2.5+n)H_2O(1.5 + m)CaO \cdot SiO_2 (1+m+n)H_2O +(1.5 - m)Ca(OH)_2.$$
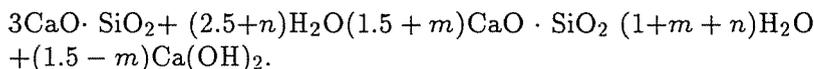
$Ca(OH)_2$: (portlandite) formed by this reaction loses water at around 450 °C. The loss of weight can be measured exactly and may serve useful information about the hydration process especially in the early phase of the reaction. TG curves can only serve realistic values if structural water does not desorb between 400 − 500 °C.

$CaCO_3$ originating from the carbonization of $Ca(OH)_2$ loses 1 mole of CO_2 between 670 − 860 °C.

The hardly crystallised C–S–H gel formed during the hydration of C_3S has similar structure as tobermorite.

Tobermorite: $5CaO \cdot 6SiO_2 \cdot 5H_2O$ loses its crystal water between 450 − 650 °C. The mole ratio between CaO and SiO_2 may increases from 0.8 − 1.5 to 1.5 − 2.0 in C–S–H gel during hydration.

The loss of weight calculated from the TG curves of the derivatograms of different samples shows that the hydration rate was lower in samples stored in 65% relative humidity than the ones stored in 100% relative humidity atmosphere. Steaming did not cause significant differences.

3.10. C_3S–$NaCl$–Water System

NaCl added to C_3S increases the hydration rate. This effect is most significant in the first phase of the process. This effect could not be observed in case of samples sprayed or spilled with NaCl solution. Samples stored in NaCl solution and samples containing NaCl both show separated and not enlarged peaks between $580 - 630$ °C. However, these peaks appear at steamed samples as well, therefore they are not caused by any chloridous hydrate. Even X-ray diffraction analysis did not detect any sign of chloride building into the crystal structure of calcium-silicate-hydrate. C–S–H gels themselves did not show recordable reflections due to their low level of crystallisation. We could only identify original C_3S, portlandite and calcite.

The explanation for the difference between the effect of NaCl to increase the hydration rate of samples containing NaCl and samples undergoing surface treatment after 1 and 28 days is the following; while NaCl dissolved in mixing water enters the system as active or free chloride, chlorides sprayed or spilled onto the C–S–H gel mainly adsorb right on the surface. In case of samples stored in NaCl solution the level of NaCl penetration into the inside of C–S–H gel is determined by the diffusion conditions. The amount of bound chloride depends on the ratio between C:S and between H:S as well.

All C_3S samples stored in NaCl solution or exposed to surface treatment show an increase in the water content.

4. Conclusion

1. During the hydration of the C_3A–water system the hexagonal calcium-aluminate-hydrates formed in the first phase of the process transformed into C_3AH_6, but C_4AH_{13} was still detected in 180-days-old samples.

2. Friedel salt appeared in hydrated C_3A samples as a result of 2% NaCl added to the mixing water. The salt was undetectable by thermal analysis, but was shown by X-ray diffraction.

3. Ettringite, monosulphate-hydrate, C_3AH_6, C_4AH_{13} and $Al(OH)_3$ can be detected during the hydration of C_3A–$CaSO_4 \cdot 2H_2O$ (30%) water system.

4. Calcium-aluminate-hydrate containing chloride appeared in samples of C_3A–$CaSO_4 \cdot 2H_2O$ water system either taking up NaCl through the mixing water, or being sprayed or spilled by 10% NaCl solution on their surface, but most significantly and convincingly in the case

of samples stored in 10% NaCl solution. The presence of Friedel salt was proved both by thermal analysis and by X-ray diffraction.

5. Cl^- from NaCl can build into already settled concrete structures as well, probably by substituting the anions of one of the AF_m phases.

6. The rate of the hydration process and the quantity of bound water is lower in samples stored in atmospheres with 65% of relative humidity, but the range of reaction products remained the same.

7. DTG curves of samples steamed for 6 hours on 80 °C and stored in 65% relative humidity afterwards show hardly any changes in the relative and absolute peak levels between $1 - 90$ days.

8. In case of lower $CaSO_4 \cdot 2H_2O$ content (20% instead of 30%) C_3AH_6 reaches higher concentrations compared to ettringite and monosulphate.

9. The exothermic peak appearing at 600 °C on the DTA curve of hydrated C_3A samples containing gypsum seems to be in connection with some intermediary structures appearing in the beginning of the hydration process, because the peak was either undetectable or insignificantly flattened after the age of 28 days.

10. The carbonate peak appearing at 770 °C on the DTG-curve disappeared after 1 day in samples containing 2% NaCl, and in samples exposed to surface treatment with 10% NaCl solution, after $28 - 56$ days showing a possible carbonate build-in into ettringite.

11. C_4AF binds chlorides in the form of monochloro-aluminate-hydrate (Friedel salt) or monochloro-ferrite-hydrate. Analogous aluminate and ferrite hydrates form solid solution with each other.

12. Neither thermal analysis nor X-ray diffraction analysis showed any sign of calcium-chloro-silicate or calcium-chloro-silicate-hydrate in hydrated C_3S samples. However, all samples containing or treated with NaCl showed an increase in their water content. The hydration in the beginning phase of the reaction was reasonably fast in C_3S samples containing NaCl.

5. Summary

Thermal and X-ray diffraction analysis showed that the chloride ion either from NaCl added to the mixing water or from outer source into the already settled cement may be bound in the presence of either C_3A or C_4AF to form $C_3A \cdot CaCl_2 \cdot H_{10}$, or may be formed from monosubstituted hexagonal hydrates: $[C_3A \cdot Ca(OH)_2 \cdot H_{12}, \ C_3F \cdot Ca(OH)_2 \cdot H_{12}, \ C_3A \cdot CaSO_4 \cdot H_{12}, C_3F \cdot CaSO_4 \cdot H_{12}]$ formerly transformed from calcium-aluminates, by substituting their anions.

Chlorous calcium-silicate-hydrates did not appear. However, we observed the effect of NaCl added to C_3S on increasing the hydration rate – mostly in the beginning of the reaction.

Acknowledgement

References

1. FRIEDEL, G. (1943): *Bull. Soc. Franc. Mineralogie* (Ref.: KÜHL H, 1961). Zement Chemie III. Band., VEB Verlag Technik, Berlin, pp. 223–262.
2. LEA, F. M. (1974): The Chemistry of Cement and Concrete. Glasgow, Bell and Bain Ltd, p. 182.
3. TAYLOR, H. F. W. (1990): Cement Chemistry, London, Academic Press, p. 182.
4. BALÁZS, GY. (1963): Betonszilárdítás a gőzölés és kalcium-klorid együttes alkalmazásával. Kandidátusi értekezés. (Solidification of Concrete by the Application of Both Steam Curing and Calcium-Chloride. Dissertation) Budapest, BME Építőanyagok Tanszék, p. 93.'
5. TENOUTASSE, N. (1967): Untersuchungen über Kinetik der Hidration des Trikalziumaluminates in Gegenwart von Kalziumsulfat und Kalziumchlorid. *Zement-Kalk-Gips,* Vol. 10. pp. 459–467.
6. CUBAUD, J. – MURAT, M. – EYRAUD, C. (1968): Etude par radiocristallographie et analyse thermique differentielle du ciment portland artificiel dopé en chlorure de calcium. *Rev. Mat.,* Vol. 639. pp. 485–496.
7. SCHWIETE, A. F. – LUDWIG, U. – ALBRECK, J. (1969): Bindung, von Kalziumchlorid und Kalziumsulfat bei der Hydratation der aluminatisch-ferritischen Klinkerbe stand-teile. *Zement-Kalk-Gips,* Vol. 5, pp. 225–235.
8. LEWITAS, J. (1955): Przyspieszenie dorjzewania betonow na budowie przy stosowaniu roznych gatunkow cementu i srodkow chemicznych. *Budownictwo Przemyslowe,* Vol. 9, pp. 15–16.
9. SZERB-SZERBINA, N. N. – SZAVRINA, JU. A. – ZSURINA, V. SZ. (1956): Obrazovanie gidrohloraljuminatov kalcija i vlijanie ih na sztrukturu cementnogo kamnja. *Dokladii Akad. Nauk. SzSzSzR.,* Vol. VIII. pp. 659–662.
10. BOROS, J-NÉ – BALÁZS, GY. (1972): C_3A–$CaSO_4$–$CaCl_2$–H_2O rendszer hidratációja. (The Hydration of C_3A–$CaSC_4$–$CaCl_2$–H_2O System) *Tudományos közlemények* Vol. 6. Budapest BME Építőanyagok Tanszék, pp. 1–105.
11. BEAUDOIN, J. J. – RAMACHANDRAN, V. S. – FELDMANN, R. F. (1990): Interaction of Chloride and C–S–H. *Cem. and Concr. Res.,* Vol. 20, pp. 875–883.
12. KUZEL, H. J. – PÖLMANN, H. (1991): Hydration of C_3A in the Presence of $Ca(OH)_2$, $CaSO_4 \cdot 2H_2O$ and $CaCO_3$. *Cem. and Concr. Res.,* Vol. 20. pp. 885–895.
13. COLLEPARDI, M. – BALDINI, G. – PAURI, M. (1978): Tricalcium-Aluminate Hydration in the Presence of Lime, Gypsum or Sodium Sulphate. *Cem. and Concr, Res.,* Vol. 8, pp. 571–580.
14. LEA, F. M. (1970): The Chemistry of Cement and Concrete. Glasgow, Bell and Bain Ltd, p. 180.